Mechanistic study of charge separation in a non-fullerene organic donor-acceptor blend using multispectral multidimensional spectroscopy

Yin Song^{1,†}, Xiao Liu^{2,†‡}, Yongxi Li², Hoang Huy Nguyen¹, Rong Duan⁴, Kevin J. Kubarych⁴, Stephen R. Forrest^{1,2,3} and Jennifer P. Ogilvie¹

¹Department of Physics, University of Michigan, Ann Arbor, MI, 48109, United States

²Department of Electrical Engineering and Computer Science, University of Michigan, Ann

Arbor, MI, 48109, United States

³Department of Material Science and Engineering, University of Michigan, Ann Arbor, MI, 48109, United States

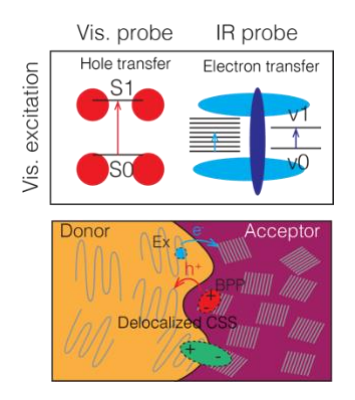
⁴Department of Chemistry, University of Michigan, Ann Arbor, MI, 48109, United States

† These authors contributed equally to this work.

Abstract: Organic photovoltaics (OPVs) based on non-fullerene acceptors are now approaching commercially viable efficiencies. One key to their success is efficient charge separation with low potential loss at the donor-acceptor heterojunction. Due to the lack of spectroscopic probes, open questions remain about the mechanisms of charge separation. Here we study charge separation of a model system comprised of the donor, poly[(2,6-(4,8-bis(5-(2-ethylhexyl)thiophen-2-yl)-benzo[1,2-b:4,5-b']dithiophene))-alt-(5,5-(1',3'-di-2-thienyl-5',7'-bis(2-ethylhexyl)benzo[1',2'-

c:4',5'-c']dithiophene-4,8-dione) (PBDB-T), and the non-fullerene acceptor, 3,9-bis(2-methylene-(3-(1,1-dicyanomethylene)-indanone))-5,5,11,11-tetrakis(4-hexylphenyl)-dithieno[2,3-d:2',3'-d']-s-indaceno[1,2-b:5,6-b']dithiophene (ITIC), using multidimensional spectroscopy spanning the visible to the mid-infrared. We find that bound polaron pairs (BPPs) generated within ITIC domains play a dominant role in efficient hole transfer, transitioning to delocalized polarons within 100 fs. The weak electron-hole binding within the BPPs and the resulting polaron delocalization are key factors for efficient charge separation at nearly zero driving force. Our work provides useful insight into how to further improve the power conversion efficiency in OPVs.

TOC Graphic



KEYWORDS Organic photovoltaics, non-fullerene acceptors, multidimensional spectroscopy, ultrafast dynamics, charge separation

Organic photovoltaics (OPVs) comprising donor-acceptor blended heterojunctions (HJ) have attracted great attention owing to rapid improvements in their power conversion efficiency that now exceed 17% ¹⁻⁷. Photoexcitation of organic material in the blend generates a tightly bound exciton. Following exciton diffusion to a nearby HJ, charge separation via electron transfer from the donor to the acceptor, or hole transfer from acceptor to donor, is achieved. Efficient charge

separation is often accompanied by a significant energy loss⁸. Recently, it has been found that near-unity charge separation efficiency can also be realized in low energy-loss junctions where the offset between the highest occupied molecular orbitals (HOMO) or lowest unoccupied MO (LUMO) is close to zero^{1, 2, 9-13}. The junctions are often comprised of conjugated polymers with electron-withdrawing groups and electron-donating groups (termed donor-acceptor (D-A) conjugated polymers), and non-fullerene acceptors (NFAs) that contain an electron-donating group with symmetrically disposed electron withdrawing groups terminating each end ^{2, 14-16}. A low energy offset, which often leads to a trade-off between current and voltage due to the reduction of the charge separation yield, does not appear to be a detriment in NFA-based OPVs. Thus a mechanistic understanding of the charge separation process in NFA-based D-A blends is essential. While a number of mechanisms have been proposed to explain ultrafast charge separation via electron transfer with a large energy offset (i.e., > 0.4 eV)^{12, 17-27}, hole transfer in the NFA-based OPVs remains poorly understood. It is remarkable that near-unity and ultrafast charge separation can be achieved with a nearly zero energy offset at the HJs in NFA-based OPVs^{10, 28}. Recently, several studies^{10, 29-34} have sought to explain efficient charge separation in these systems. By estimating the electron-hole separation distance using the Stark shift, Tamai, et al.³³ showed that excitons can rapidly dissociate into the delocalized charge transfer states in blends comprising pervlene diimide (PDI) dimer acceptors. Niu et al. reported that charge separation is mediated by weakly bound excitons in an NFA-based blend. 35,36 Recently, Wang et al. 29 reported that an intramoiety intermediate state in the acceptor domain acts as the only precursor for charge separation via hole transfer in organic donor-NFA blends, where hole transfer is much slower than the formation of the intermediate state. Whether this intermediate state is an excimer, or a bound polaron pair (BPP) remains to be determined. 29, 35, 37-39

To elucidate the charge separation mechanism and identify the nature of the intermediate states, a combination of two-dimensional electronic spectroscopy (2DES) and twowe applied dimensional electronic-vibrational spectroscopy (2DEV, or 2D visible-mid-IR spectroscopy)^{40, 41} to study an archetypal blend comprised of the donor, poly[(2,6-(4,8-bis(5-(2-ethylhexyl)thiophen-2-yl)-benzo[1,2-b:4,5-b']dithiophene))-alt-(5,5-(1',3'-di-2-thienyl-5',7'-bis(2ethylhexyl)benzo[1',2'-c:4',5'-c']dithiophene-4,8-dione)] (PBDB-T), and the acceptor 3,9-bis(2methylene-(3-(1,1-dicyanomethylene)-indanone))-5,5,11,11-tetrakis(4-hexylphenyl)dithieno[2,3-d:2',3'-d']-s-indaceno[1,2-b:5,6-b']dithiophene (ITIC) (Figure 1a and Figure S1a). The OPV device made of this blend exhibits a decent power conversion efficiency of >11% and excellent thermal stability^{1, 42}. In 2D spectroscopy, a sequence of two pump pulses prepare an excited-state population, the evolution of which is monitored as a function of waiting time T by a probe pulse. The 2D spectrum is a frequency-frequency map that correlates ultrafast dynamics of photoexcited and photoproduct states and reveals the photoexcited dynamics by its spectral evolution. 40, 41, 43-45 2D spectroscopy is closely related to transient absorption (or pump-probe) spectroscopy but provides an additional dimension, resolving ultrafast dynamics with respect to the excitation frequency. Here we used a multispectral combination of 2DES to probe hole transfer, and 2DEV to reveal electron transfer and the formation of charge separation intermediates. 40, 43 The complementary information obtained reveals both the nature of the intermediate state and the charge separation mechanism, providing insight for the design of improved OPV materials.

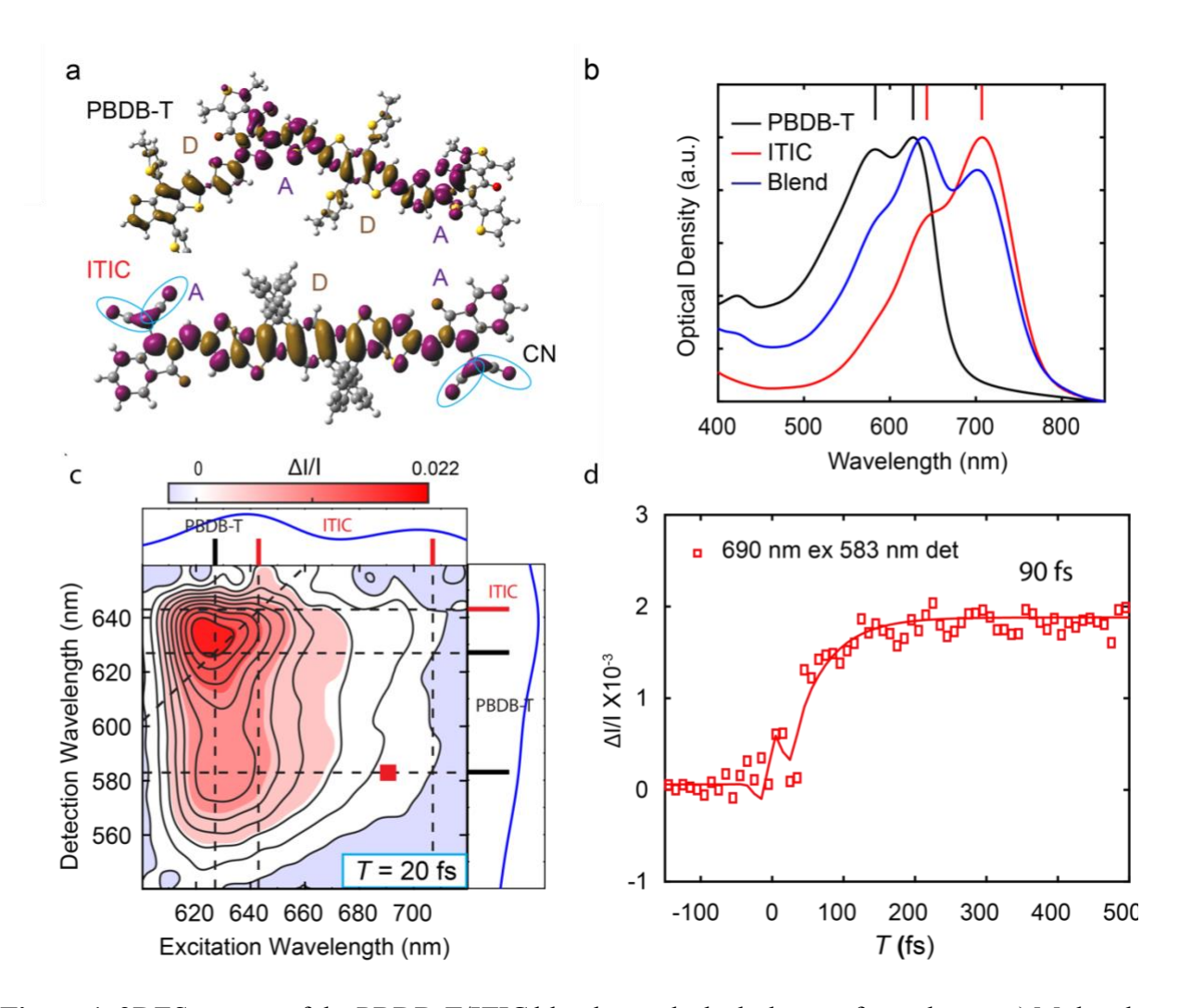


Figure 1: 2DES spectra of the PBDB-T/ITIC blend reveals the hole transfer pathway. a) Molecular structures of PBDB-T and ITIC, along with charge density distributions of the lowest singlet state calculated by TD-DFT. The electron and the hole density distributions are purple and yellow, respectively. Nitrile groups (CN) are circled in blue. b) Absorption spectra of neat PBDB-T film, neat ITIC film and the PBDB-T/ITIC blend. The lines in the plot indicate two lowest vibronic transitions (0-0 and 0-1) of PBDB-T (black) and ITIC (red). c) 2DES absorptive spectrum of the PBDB-T/ITIC blend at 20 fs under excitation from wavelengths of 600-720 nm and probed from 540 to 660 nm. The absorption spectra are shown at the top and to the right of the 2DES spectrum. The vertical and horizontal dashed lines in the 2DES spectrum and the lines in the absorption spectra indicate peak positions. Contour intervals: 10% of the maximum amplitude. d) Time response (square: the experimental data; line: the exponential fits) of the cross peak revealing the hole transfer dynamics. The corresponding peak position is illustrated with a red square box in (c).

Figure 1b shows absorption spectra of neat PBDB-T film, neat ITIC film and their blend. The 0-0 and 0-1 vibronic transitions of PBDB-T (or ITIC) are peaked at 627 nm and 583 nm (or 707 nm

and 643 nm), respectively. The absorption spectrum of the blend is a linear combination of two neat films. To investigate charge separation via hole transfer, we performed 2DES using separate pump and probe pulses with spectra (Figure S1b) covering the absorption of ITIC and PBDB-T, respectively. The experimental details can be found in Section S1 of the Supporting Information (SI). The pulse energies of the pump beams were kept low enough to avoid second-order kinetic processes as shown in Figure S2-S4. Figure 1c depicts the 2DES spectrum of the blend at 20 fs, exhibiting a pattern of diagonal and cross peaks (λ_{ex} , λ_{det}) that correspond to the 0-0 and 0-1 vibronic transitions of ITIC and PBDB-T. The 2DES data are presented as $\Delta I/I$ because the experiments were performed in the BOXCARS geometry where the signal is generated in a distinct phase-matched direction from the pump and probe pulses and is interfered with a local oscillator to optimize the signal-to-noise ratio⁴⁶. This is in contrast to transient absorption spectroscopy and 2D spectroscopy in the pump-probe geometry where the probe pulse copropagates with the signal and acts as the local oscillator, making $\Delta T/T$ appropriate. While there is a scaling factor between $\Delta I/I$ and $\Delta T/T$, $\Delta I/I$ carries the same information and can be viewed as $\Delta T/T$ in the current work. The cross peaks at $(\lambda_{ex}, \lambda_{det}) = (643 \text{ nm}, 583 \text{ nm})$ and $(\lambda_{ex}, \lambda_{det}) = (707 \text{ nm}, 627 \text{ nm})$ stem from the ground-state bleaching (GSB) of the PBDB-T under photoexcitation of ITIC, and thus reveal the hole transfer dynamics. Due to the spectral overlap of PBDB-T and ITIC from 600 to 680 nm, and low signal at 707 nm, we examine dynamics at cross peak locations where there is better spectral separation between donor and acceptor (λ_{ex} , λ_{det}) = (690 nm, 583 nm), as shown in Figure 1d. The exponential fit of the time response shows a peak rise time corresponding to hole transfer of 90 \pm 20 fs.

Hole transfer can occur either via direct dissociation of a localized exciton at the donor-acceptor HJ, or via an intermediate state (i.e. an excimer or a BPP). Previously, we have studied charge

separation via efficient exciton dissociation using time-resolved photoluminescence³⁶. Here we use 2DEV to determine if and how an intermediate state contributes to hole transfer. In this experiment, we excite the 640 to 720 nm region, spanning the S0→S1 transition and vibronic shoulders of ITIC and probe the 2130 to 2270 cm⁻¹ region covering the symmetric nitrile (CN) stretching mode of ITIC. As shown in Figure 2a, the 2DEV spectrum of the neat ITIC film averaged from 50 to 150 fs after photoexcitation exhibits a vibrational peak at 2219 cm⁻¹ corresponding

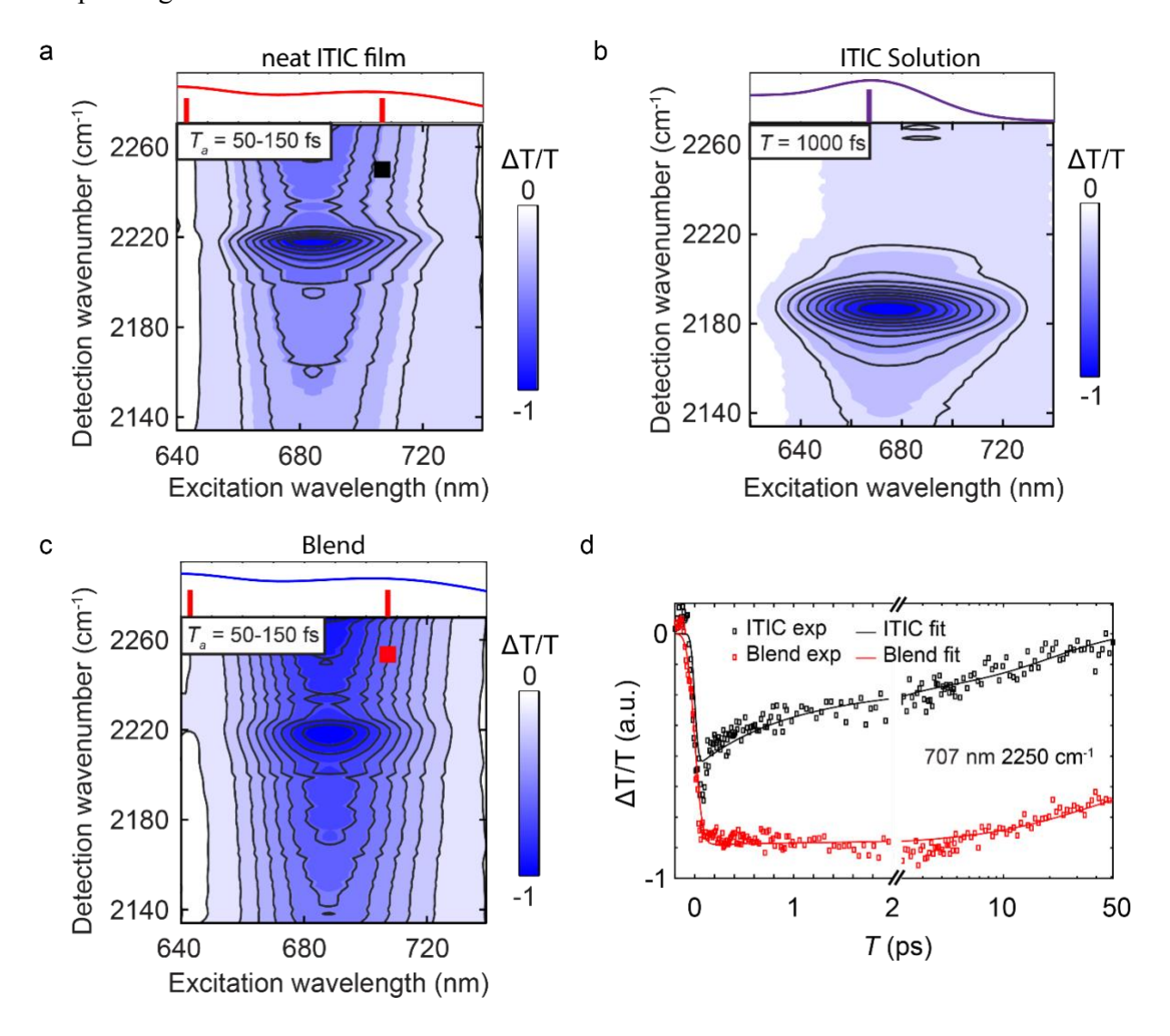


Figure 2 2DEV spectra probe charge separation via electron transfer in the PBDB-T/ITIC blend. a) 2DEV spectrum of a neat ITIC film averaged from T = 50 to 150 fs. b) 2DEV spectrum of the

ITIC in chlorobenzene solution at T = 1000 fs. c) 2DEV spectrum of the PBDB-T/ITIC blend averaged from T = 50 to 150 fs. d) Time responses of the broadband PA with $\lambda_{ex} = 707$ nm and $v_{det} = 2250$ cm⁻¹ in the neat ITIC film (black squares) and the blend (red squares). Solid lines show exponential fits to the data. Contour levels: -1:0.1:0 of the maximum amplitude.

to the CN stretching mode of the ITIC. The dominance of excited state absorption (ESA) of the CN vibrational peak over GSB suggests that charge transfer occurs within neat ITIC film, giving rise to the ITIC anion. This is rationalized by the fact that the extinction coefficient of the CN stretching mode of the ITIC anion is about 1000 times stronger than that of its neutral counterpart (Figure S5). On top of the CN peak is a broad, photoinduced absorption (PA) band which arises and decays with the CN vibrational peak. Previous studies have shown that the broadband PA in the mid-IR can be attributed to excited states with charge transfer character such as delocalized polarons⁴⁷⁻⁴⁹, BPPs⁵⁰, and excimers⁵¹. In our case, the assignment to an excimer can be ruled out by the observation of the CN peak from the ITIC anion. We find that the broadband PA decays biexponentially with time constants of 2.2±0.8 ps (52%) and 31±8 ps (48%). The short lifetime of the PA is consistent with it arising from BPPs rather than long-lived polarons which typically have lifetimes of ns⁵². Furthermore, we find that the broadband PA is not observed in the 2DEV of the ITIC solution as shown in Figure 2b, suggesting that the bound polaron pairs are intermolecular species. We note that the CN peak in solution appears at a lower frequency than the neat ITIC film. This observation can be rationalized by the charge delocalization in the film in accordance with previous studies^{53, 54}. A similar combination of CN vibrational peak and broadband PA are also observed in the 2DEV spectrum of the blend in Figure 2c. Unlike the neat ITIC film, only a small fraction (28%) of the PA in the blend decays with a time constant of 27±6 ps (Figure 2d), whereas the balance remains for nanoseconds. The long-lived PA provides evidence for the formation of the charge separated states or polarons. The absence of the fast decay component suggests that dissociation of the BPPs, i.e. hole transfer, occurs efficiently at the HJ, outcompeting the

recombination at ITIC domains. The 2.2 ps component, which is absent in the blend, may be attributed to the second-order reaction such as the annihilation between the BPPs, or between the BPP and the exciton, or Auger recombination, in accordance with previous studies^{55, 56}. Efficient charge separation in the blend significantly reduces the density of the BPPs and the excitons and thus prevent such loss processes.

Figures 3a and 3b display 2DEV spectra of the PBDB-T film and PBDB-T/ITIC blend, respectively, in the range of excitation wavelengths where PBDB-T is predominantly photoexcited (540 to 600 nm). In both cases, we observe broadband PA. The broadband PA in the neat PBDB-T film can be assigned to bound polaron pairs in accordance with previous studies^{50,57}, whereas in the blend, it can stem from either bound polaron pairs or delocalized polarons. In the blend, a vibrational peak at 2219 cm⁻¹ appears which we attribute to the CN stretch of the ITIC nitrile end groups that appears due to electron transfer from PBDB-T. Therefore, we use the amplitude of the CN peak to estimate the electron transfer rate. To do this, we first extract the slice 2DEV spectrum at each excitation wavelength, which is fit to a function comprised of a third-order polynomial for the PA, and a Gaussian function for the CN peak (Figure 3c). Then the amplitude change in the CN peak is fit to an exponential. We find that the CN peak rises, i.e. electron transfers, with a time constant of 80±20 fs (Figure 3c).

The time response of the broadband PA is fit by a triexponential function with time constants of 5.8 ± 1.5 ps (36%), 38 ± 13 ps (42%) and > 1 ns (22%). The small bump at time origin is attributed to the scattering and/or the coherent artifact since the mid-IR pulse duration is about 90 fs^{58, 59}. Thus this portion is not taken into account during the fit. The long-lived PA has also been observed upon excitation of ITIC aggregates and in other organic donor-acceptor blends^{48, 49} and can be assigned to the delocalized polarons generated via electron transfer. Two fast decaying

components of PA are also observed in the neat PBDB-T film^{27, 50, 57, 60} with time constants of 9 ± 3 ps (46%) and 50 ± 9 ps (54%) (Figure 3d). The similarity between the PA decay behavior in the neat PBDB-T film and PBDB-T domains of the blend, and the relatively small nanosecond decay component in the films suggests that the bound polaron pair in neat PBDB-T domain may not efficiently transition to charge separated states at the HJ as they do in NFA domains, but rather play only a minor role in charge separation.

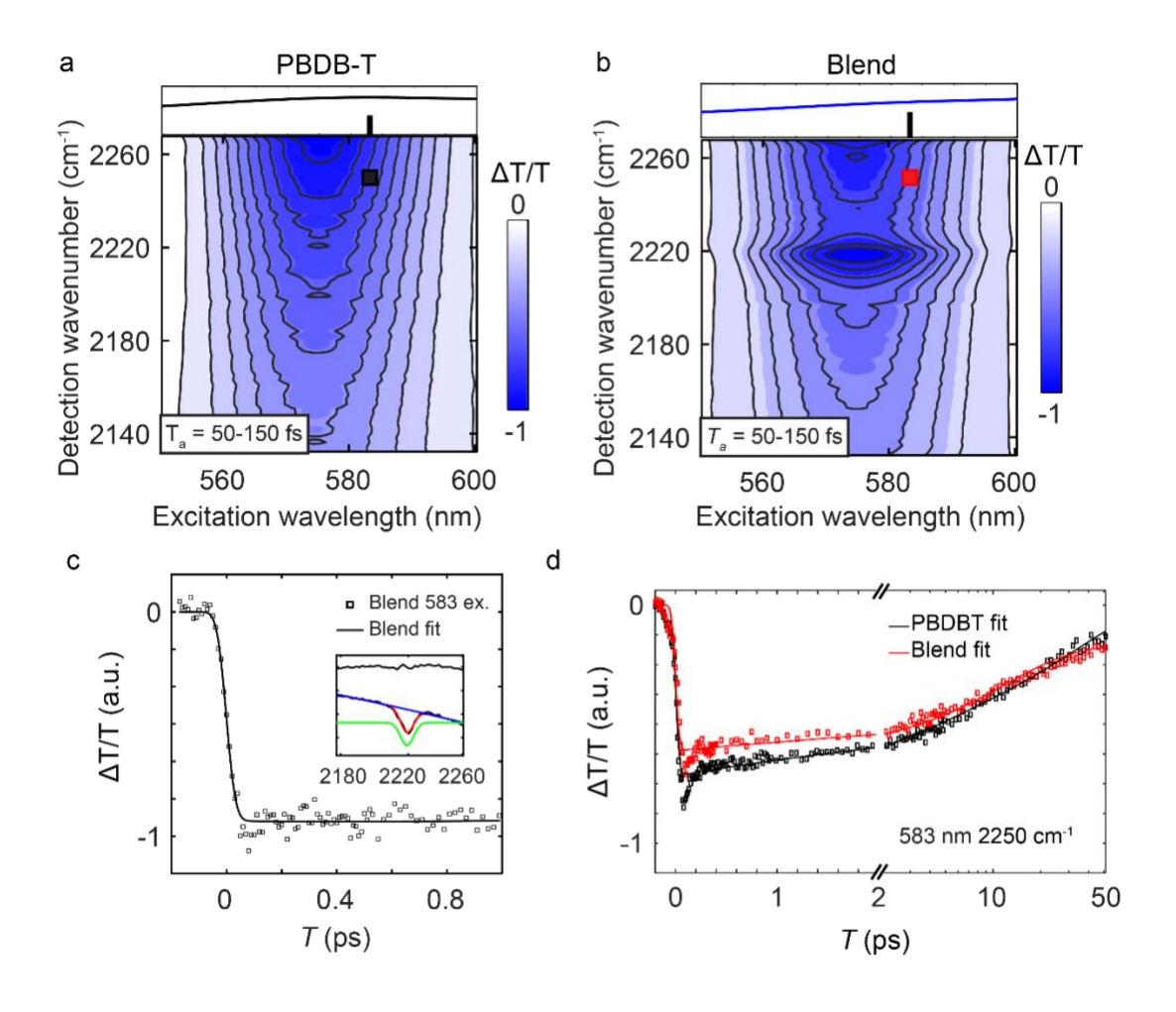


Figure 3 2DEV probes electron transfer and charge separation in the PBDB-T/ITIC blend. a) 2DEV spectrum of neat PBDB-T film averaged from T = 50 to 150 fs. b) 2DEV spectrum of the blend film averaged from T = 50 to 150 fs. c) Time response of the vibrational peak from the CN stretching mode (black squares) upon $\lambda_{ex} = 583$ nm and its exponential fit (black line). The inset shows the fit of the transient spectrum using a sum of a Gaussian function (for the vibrational peak) and a polynomial (for the polaron absorption). d) Time responses of the broadband photoinduced absorption with $\lambda_{ex} = 583$ nm and $v_{det} = 2250$ cm⁻¹ in neat PBDB-T film (black squares) and the

blend (red squares). The exponential fits are shown by the solid lines. Contour levels: -1:0.1:0 of the maximum amplitude.

Our experiments reveal sub-100 fs electron transfer and hole transfer in the PBDB-T/ITIC blend. We find that an intermediate state with strong charge transfer character in the ITIC domains acts as a precursor for the efficient hole transfer process, while such an intermediate may play a relatively minor role in the electron transfer pathway. The strong charge transfer character of the intermediate is evident by the observation of the CN vibrational peak from the ITIC anion, which is consistent with previous studies by Miller, et al.^{53, 61, 62} Furthermore, the 2DEV spectra of neat ITIC film and the blend exhibit broadband PA immediately following photoexcitation. This broadband PA cannot be attributed to Frenkel excitons since they often absorb in visible or near-IR⁵⁰. The 2DEV spectrum of ITIC in solution does not exhibit such a broadband PA in the mid-IR either, which confirms that this feature is not from ESA of the single ITIC molecule. In contrast, previous studies have shown that broadband PA in the mid-IR can be attributed to excited states with charge transfer character such as delocalized polarons⁴⁷⁻⁴⁹, BPPs⁵⁰, and excimers⁵¹. In our case, the assignment to an excimer can be ruled out by the observation of the CN peak from the ITIC anion. The short lifetime of the PA (2.2±0.8 ps and 31±8 ps) in neat ITIC film indicates that the broadband PA is more likely to be from a BPP than long-lived polarons (typically with a lifetime of ns). The absence of the fast decay of PA in the blend suggests that these BPPs efficiently transition to the charge separated state in the blend. Considering the discussion above, we conclude that BPPs are generated in ITIC domains and contribute to the hole transfer pathway. We note that the relative strengths of the CN peak and the broadband PA shown in Figures 2 and 3 are different in the neat films and blends due to the different relative populations and oscillator strengths of the contributing species.

Coulomb attraction in BPPs is much weaker than that in Frenkel excitons^{27, 30, 50, 60}, which can significantly enhance the charge separation rate at the HJ with small energy offset. The loosely bound polaron pair or charge transfer state has also been observed in fullerene films^{63, 64} while its contribution to charge separation has not been fully explored. This is probably due to the energy offset between organic donor and fullerene that is often large enough to overcome the Coulomb attraction even without the assistance of the BPP. However, this effect may not be neglected in the NFA-based OPVs due to the small energy offset and can be utilized to further reduce the energy loss during charge separation. Furthermore, as inferred from the broadband PA signal of ITIC aggregates and the blend in Fig. 2, BPPs and polarons in the blend are delocalized, which could further reduce the Coulomb attraction and potentially increase the charge separation rate. TD-DFT calculations also showed that the CN peak of the ITIC anion is red shifted by a 20 cm⁻¹ as compared to in neutral and cationic ITIC. Such a peak shift is absent in our experiments. However, previous studies have shown that the peak shift can be significantly reduced when the charge is delocalized⁵³. Thus the absence of observed peak shift may be a result of the delocalization of the negative charge in the ITIC film. We have previously suggested that the rapid formation of the delocalized negative charges in the ITIC film may be facilitated by the strong charge-transfer character and weak electron-hole binding energy in the excited state of an isolated ITIC molecule³⁶. Thus we conclude that both the weak Coulomb attraction in the BPP and its delocalization may play important roles in efficient hole transfer at small energy offset.

In summary, multispectral 2D spectroscopy with visible and mid-IR probes has provided insight into the charge separation mechanism in an archetypal NFA blend heterojunction (PBDB-T/ITIC). Rapid hole transfer from ITIC to PBDB-T and electron transfer from PBDB-T to ITIC have been revealed by 2DES and 2DEV, respectively. Detailed analysis of 2DEV spectra show that BPPs in

the ITIC domain are key precursors for charge separation via hole transfer and are efficiently

converted to delocalized polarons at the heterojunction on the time scale of ~ 100 fs. However,

BPPs in the PBDB-T domain quickly relax to the ground state and thus localized excitons act as

the dominant precursor for charge separation via electron transfer. The fast charge separation at

small HOMO offset is facilitated by both the weak Coulomb attraction in the BPPs and the

delocalization of polarons. Our findings highlight the importance of the synergistic effect of BPPs

and delocalization, providing an important strategy for optimizing the charge separation efficiency

in organic donor-acceptor blend heterojunctions with a low potential offset.

ASSOCIATED CONTENT

Supporting information

Experimental Methods; Pump and probe spectra in the 2DES and 2DEV; Fluencedependent study; TD-DFT calculations; Pump pulse compression; Time-resolved

photoluminescence.

This material is available free of charge via the Internet at http://pubs.acs.org.

AUTHOR INFORMATION

Corresponding Author: jogilvie@umich.edu

Present Addresses

‡ Department of Electrical Engineering, Princeton University, Princeton, NJ 08544, United

States

Author Contributions

The manuscript was written through contributions of all authors. All authors have given approval

to the final version of the manuscript.

Funding Sources

Y.S., S.F. and J.P.O. acknowledge the support of the National Science Foundation through instrumentation grant #CHE-1428479 and grant #DMR-1905401. Y.S. acknowledges the support of the Natural Sciences and Engineering Council of Canada (NSERC) for a Postdoctoral

Fellowship.

13

Notes

The authors declare no competing financial interest.

ACKNOWLEDGMENT

Y.S. thank Dr. Ryan Pensack and Dr. Christopher Grieco for the insightful discussion on the sample preparations and spectroscopic measurements.

References:

- 1. Zhao, W.; Qian, D.; Zhang, S.; Li, S.; Inganas, O.; Gao, F.; Hou, J., Fullerene-Free Polymer Solar Cells with over 11% Efficiency and Excellent Thermal Stability. *Adv Mater* **2016**, *28* (23), 4734-9.
- 2. Hou, J.; Inganas, O.; Friend, R. H.; Gao, F., Organic solar cells based on non-fullerene acceptors. *Nat Mater* **2018**, *17* (2), 119-128.
- 3. Li, Y.; Zhong, L.; Gautam, B.; Bin, H.-J.; Lin, J.-D.; Wu, F.-P.; Zhang, Z.; Jiang, Z.-Q.; Zhang, Z.-G.; Gundogdu, K.; Li, Y.; Liao, L.-S., A near-infrared non-fullerene electron acceptor for high performance polymer solar cells. *Energy & Environmental Science* **2017**, *10* (7), 1610-1620.
- 4. Zhan, L. L.; Li, S. X.; Lau, T. K.; Cui, Y.; Lu, X. H.; Shi, M. M.; Li, C. Z.; Li, H. Y.; Hou, J. H.; Chen, H. Z., Over 17% efficiency ternary organic solar cells enabled by two non-fullerene acceptors working in an alloy-like model. *Energy & Environmental Science* **2020**, *13* (2), 635-645.
- 5. Cui, Y.; Yao, H. F.; Hong, L.; Zhang, T.; Tang, Y. B.; Lin, B. J.; Xian, K. H.; Gao, B. W.; An, C. B.; Bi, P. Q.; Ma, W.; Hou, J. H., Organic photovoltaic cell with 17% efficiency and superior processability. *Natl Sci Rev* **2020**, *7* (7), 1239-1246.
- 6. Lin, Y. B.; Adilbekova, B.; Firdaus, Y.; Yengel, E.; Faber, H.; Sajjad, M.; Zheng, X. P.; Yarali, E.; Seitkhan, A.; Bakr, O. M.; El-Labban, A.; Schwingenschlogl, U.; Tung, V.; McCulloch, I.; Laquai, F.; Anthopoulos, T. D., 17% Efficient Organic Solar Cells Based on Liquid Exfoliated WS2 as a Replacement for PEDOT:PSS. *Advanced Materials* **2019**, *31* (46).
- 7. Meng, L.; Zhang, Y.; Wan, X.; Li, C.; Zhang, X.; Wang, Y.; Ke, X.; Xiao, Z.; Ding, L.; Xia, R.; Yip, H.-L.; Cao, Y.; Chen, Y., Organic and solution-processed tandem solar cells with 17.3% efficiency. *Science* **2018**, *361* (6407), 1094.
- 8. Menke, S. M.; Ran, N. A.; Bazan, G. C.; Friend, R. H., Understanding Energy Loss in Organic Solar Cells: Toward a New Efficiency Regime. *Joule* **2018**, *2* (1), 25-35.
- 9. Sun, C.; Qin, S.; Wang, R.; Chen, S.; Pan, F.; Qiu, B.; Shang, Z.; Meng, L.; Zhang, C.; Xiao, M.; Yang, C.; Li, Y., High Efficiency Polymer Solar Cells with Efficient Hole Transfer at Zero Highest Occupied Molecular Orbital Offset between Methylated Polymer Donor and Brominated Acceptor. *J Am Chem Soc* **2020**, *142* (3), 1465-1474.
- 10. Zhong, Y. F.; Causa', M.; Moore, G. J.; Krauspe, P.; Xiao, B.; Gunther, F.; Kublitski, J.; Shivhare, R.; Benduhn, J.; BarOr, E.; Mukherjee, S.; Yallum, K. M.; Rehault, J.; Mannsfeld, S. C. B.; Neher, D.; Richter, L. J.; DeLongchamp, D. M.; Ortmann, F.; Vandewal, K.; Zhou, E.; Banerji, N., Sub-picosecond charge-transfer at near-zero driving force in polymer:non-fullerene acceptor blends and bilayers. *Nat Commun* **2020**, *11* (1).
- 11. Li, S.; Zhan, L.; Sun, C.; Zhu, H.; Zhou, G.; Yang, W.; Shi, M.; Li, C. Z.; Hou, J.; Li, Y.; Chen, H., Highly Efficient Fullerene-Free Organic Solar Cells Operate at Near Zero Highest Occupied Molecular Orbital Offsets. *J Am Chem Soc* **2019**, *141* (7), 3073-3082.
- 12. Perdigon-Toro, L.; Zhang, H. T.; Markina, A. S.; Yuan, J.; Hosseini, S. M.; Wolff, C. M.; Zuo, G. Z.; Stolterfoht, M.; Zou, Y. P.; Gao, F.; Andrienko, D.; Shoaee, S.; Neher, D., Barrierless Free Charge

- Generation in the High-Performance PM6:Y6 Bulk Heterojunction Non-Fullerene Solar Cell. *Advanced Materials* **2020**, *32* (9).
- 13. Liu, X.; Rand, B. P.; Forrest, S. R., Engineering Charge-Transfer States for Efficient, Low-Energy-Loss Organic Photovoltaics. *Trends in Chemistry* **2019**, *1* (9), 815-829.
- 14. Zhang, G.; Zhao, J.; Chow, P. C. Y.; Jiang, K.; Zhang, J.; Zhu, Z.; Zhang, J.; Huang, F.; Yan, H., Nonfullerene Acceptor Molecules for Bulk Heterojunction Organic Solar Cells. *Chem Rev* **2018**, *118* (7), 3447-3507.
- 15. Cheng, P.; Li, G.; Zhan, X.; Yang, Y., Next-generation organic photovoltaics based on non-fullerene acceptors. *Nature Photonics* **2018**, *12* (3), 131-142.
- 16. Lopez, S. A.; Sanchez-Lengeling, B.; de Goes Soares, J.; Aspuru-Guzik, A., Design Principles and Top Non-Fullerene Acceptor Candidates for Organic Photovoltaics. *Joule* **2017**, *1* (4), 857-870.
- 17. Hood, S. N.; Kassal, I., Entropy and Disorder Enable Charge Separation in Organic Solar Cells. *J Phys Chem Lett* **2016**, *7* (22), 4495-4500.
- 18. Grancini, G.; Maiuri, M.; Fazzi, D.; Petrozza, A.; Egelhaaf, H. J.; Brida, D.; Cerullo, G.; Lanzani, G., Hot exciton dissociation in polymer solar cells. *Nature Materials* **2013**, *12* (1), 29-33.
- 19. Jailaubekov, A. E.; Willard, A. P.; Tritsch, J. R.; Chan, W. L.; Sai, N.; Gearba, R.; Kaake, L. G.; Williams, K. J.; Leung, K.; Rossky, P. J.; Zhu, X. Y., Hot charge-transfer excitons set the time limit for charge separation at donor/acceptor interfaces in organic photovoltaics. *Nature Materials* **2013**, *12* (1), 66-73.
- 20. Marsh, R. A.; Hodgkiss, J. M.; Friend, R. H., Direct Measurement of Electric Field-Assisted Charge Separation in Polymer: Fullerene Photovoltaic Diodes. *Advanced Materials* **2010**, *22* (33), 3672-+.
- 21. Jamieson, F. C.; Agostinelli, T.; Azimi, H.; Nelson, J.; Durrant, J. R., Field-Independent Charge Photogeneration in PCPDTBT/PC70BM Solar Cells. *J Phys Chem Lett* **2010**, *1* (23), 3306-3310.
- 22. Bakulin, A. A.; Rao, A.; Pavelyev, V. G.; van Loosdrecht, P. H. M.; Pshenichnikov, M. S.; Niedzialek, D.; Cornil, J.; Beljonne, D.; Friend, R. H., The Role of Driving Energy and Delocalized States for Charge Separation in Organic Semiconductors. *Science* **2012**, *335* (6074), 1340-1344.
- 23. Gelinas, S.; Rao, A.; Kumar, A.; Smith, S. L.; Chin, A. W.; Clark, J.; van der Poll, T. S.; Bazan, G. C.; Friend, R. H., Ultrafast Long-Range Charge Separation in Organic Semiconductor Photovoltaic Diodes. *Science* **2014**, *343* (6170), 512-516.
- 24. Jakowetz, A. C.; Bohm, M. L.; Sadhanala, A.; Huettner, S.; Rao, A.; Friend, R. H., Visualizing excitations at buried heterojunctions in organic semiconductor blends. *Nature Materials* **2017**, *16* (5), 551+.
- 25. Liu, X.; Ding, K.; Panda, A.; Forrest, S. R., Charge Transfer States in Dilute Donor-Acceptor Blend Organic Heterojunctions. *Acs Nano* **2016**, *10* (8), 7619-7626.
- 26. Falke, S. M.; Rozzi, C. A.; Brida, D.; Maiuri, M.; Amato, M.; Sommer, E.; De Sio, A.; Rubio, A.; Cerullo, G.; Molinari, E.; Lienau, C., Coherent ultrafast charge transfer in an organic photovoltaic blend. *Science* **2014**, *344* (6187), 1001-1005.
- 27. De Sio, A.; Troiani, F.; Maiuri, M.; Rehault, J.; Sommer, E.; Lim, J.; Huelga, S. F.; Plenio, M. B.; Rozzi, C. A.; Cerullo, G.; Molinari, E.; Lienau, C., Tracking the coherent generation of polaron pairs in conjugated polymers. *Nat Commun* **2016**, *7*, 13742.
- 28. Liu, J.; Chen, S.; Qian, D.; Gautam, B.; Yang, G.; Zhao, J.; Bergqvist, J.; Zhang, F.; Ma, W.; Ade, H.; Inganäs, O.; Gundogdu, K.; Gao, F.; Yan, H., Fast charge separation in a non-fullerene organic solar cell with a small driving force. *Nature Energy* **2016**, *1* (7).
- 29. Wang, R.; Zhang, C.; Li, Q.; Zhang, Z.; Wang, X.; Xiao, M., Charge Separation from an Intra-Moiety Intermediate State in the High-Performance PM6:Y6 Organic Photovoltaic Blend. *Journal of the American Chemical Society* **2020**, *142* (29), 12751–12759.
- 30. Wang, R.; Yao, Y.; Zhang, C.; Zhang, Y.; Bin, H.; Xue, L.; Zhang, Z. G.; Xie, X.; Ma, H.; Wang, X.; Li, Y.; Xiao, M., Ultrafast hole transfer mediated by polaron pairs in all-polymer photovoltaic blends. *Nat Commun* **2019**, *10* (1), 398.

- 31. Cerullo, G.; Franco, V. A. C.; Gasparini, N.; Nagahara, T.; Lüer, L.; Cerullo, G.; Brabec, C.; Ogilvie, J.; Kärtner, F.; Khalil, M.; Li, R., Instantaneous charge separation in non-fullerene acceptor bulk-heterojunction of highly efficient solar cells. *EPJ Web of Conferences* **2019**, *205*.
- 32. Baran, D.; Gasparini, N.; Wadsworth, A.; Tan, C. H.; Wehbe, N.; Song, X.; Hamid, Z.; Zhang, W.; Neophytou, M.; Kirchartz, T.; Brabec, C. J.; Durrant, J. R.; McCulloch, I., Robust nonfullerene solar cells approaching unity external quantum efficiency enabled by suppression of geminate recombination. *Nat Commun* **2018**, *9* (1), 2059.
- 33. Tamai, Y.; Fan, Y.; Kim, V. O.; Ziabrev, K.; Rao, A.; Barlow, S.; Marder, S. R.; Friend, R. H.; Menke, S. M., Ultrafast Long-Range Charge Separation in Nonfullerene Organic Solar Cells. *Acs Nano* **2017**, *11* (12), 12473-12481.
- 34. Pan, Q. Q.; Li, S. B.; Duan, Y. C.; Wu, Y.; Zhang, J.; Geng, Y.; Zhao, L.; Su, Z. M., Exploring what prompts ITIC to become a superior acceptor in organic solar cell by combining molecular dynamics simulation with quantum chemistry calculation. *Phys Chem Chem Phys* **2017**, *19* (46), 31227-31235.
- 35. Niu, M. S.; Wang, K. W.; Yang, X. Y.; Bi, P. Q.; Zhang, K. N.; Feng, X. J.; Chen, F.; Qin, W.; Xia, J. L.; Hao, X. T., Hole Transfer Originating from Weakly Bound Exciton Dissociation in Acceptor-Donor-Acceptor Nonfullerene Organic Solar Cells. *J Phys Chem Lett* **2019**, *10* (22), 7100-7106.
- 36. Liu, X.; Li, Y.; Ding, K.; Forrest, S., Energy Loss in Organic Photovoltaics: Nonfullerene Versus Fullerene Acceptors. *Physical Review Applied* **2019**, *11* (2), 024060.
- 37. Aryanpour, K.; Sheng, C. X.; Olejnik, E.; Pandit, B.; Psiachos, D.; Mazumdar, S.; Vardeny, Z. V., Evidence for excimer photoexcitations in an ordered π -conjugated polymer film. *Physical Review B* **2011**, 83 (155124), 1-5.
- 38. Reid, O. G.; Pensack, R. D.; Song, Y.; Scholes, G. D.; Rumbles, G., Charge Photogeneration in Neat Conjugated Polymers. *Chemistry of Materials* **2013**, *26* (1), 561-575.
- 39. Liu, Y.; Zuo, L.; Shi, X.; Jen, A. K. Y.; Ginger, D. S., Unexpectedly Slow Yet Efficient Picosecond to Nanosecond Photoinduced Hole-Transfer Occurs in a Polymer/Nonfullerene Acceptor Organic Photovoltaic Blend. *ACS Energy Letters* **2018**, *3* (10), 2396-2403.
- 40. Oliver, T. A. A.; Lewis, N. H. C.; Fleming, G. R., Correlating the motion of electrons and nuclei with two-dimensional electronic–vibrational spectroscopy. *Proceedings of the National Academy of Sciences* **2014**, *111* (28), 10061.
- 41. Gaynor, J. D.; Courtney, T. L.; Balasubramanian, M.; Khalil, M., Fourier transform two-dimensional electronic-vibrational spectroscopy using an octave-spanning mid-IR probe. *Opt Lett* **2016**, *41* (12), 2895-8.
- 42. Lin, Y. Z.; Wang, J. Y.; Zhang, Z. G.; Bai, H. T.; Li, Y. F.; Zhu, D. B.; Zhan, X. W., An Electron Acceptor Challenging Fullerenes for Efficient Polymer Solar Cells. *Advanced Materials* **2015**, *27* (7), 1170-1174.
- 43. Song, Y.; Konar, A.; Sechrist, R.; Roy, V. P.; Duan, R.; Dziurgot, J.; Policht, V.; Matutes, Y. A.; Kubarych, K. J.; Ogilvie, J. P., Multispectral multidimensional spectrometer spanning the ultraviolet to the mid-infrared. *Review of Scientific Instruments* **2019**, *90* (1), 013108.
- 44. Gelzinis, A.; Augulis, R.; Butkus, V.; Robert, B.; Valkunas, L., Two-dimensional spectroscopy for non-specialists. *Biochimica et Biophysica Acta (BBA) Bioenergetics* **2019**, *1860* (4), 271-285.
- 45. Song, Y.; Clafton, S. N.; Pensack, R. D.; Kee, T. W.; Scholes, G. D., Vibrational coherence probes the mechanism of ultrafast electron transfer in polymer-fullerene blends. *Nat Commun* **2014**, *5* (4933), 1-7.
- 46. Fuller, F. D.; Ogilvie, J. P., Experimental Implementations of Two-Dimensional Fourier Transform Electronic Spectroscopy. *Annu Rev Phys Chem* **2015**, *66*, 667-690.
- 47. Sheng, C. X.; Kim, K. H.; Tong, M.; Yang, C.; Kang, H.; Park, Y. W.; Vardeny, Z. V., Ultrafast Transient Spectroscopy of Trans-Polyacetylene in the Midinfrared Spectral Range. *Phys Rev Lett* **2020**, *124* (1), 017401.

- 48. Osterbacka, R.; Jiang, X. M.; An, C. P.; Horovitz, B.; Vardeny, Z. V., Photoinduced quantum interference antiresonances in pi-conjugated polymers. *Phys Rev Lett* **2002**, *88* (22), 226401.
- 49. Osterbacka, R.; An, C. P.; Jiang, X. M.; Vardeny, Z. V., Two-dimensional electronic excitations in self-assembled conjugated polymer nanocrystals. *Science* **2000**, *287* (5454), 839-842.
- 50. Tautz, R.; Da Como, E.; Limmer, T.; Feldmann, J.; Egelhaaf, H. J.; von Hauff, E.; Lemaur, V.; Beljonne, D.; Yilmaz, S.; Dumsch, I.; Allard, S.; Scherf, U., Structural correlations in the generation of polaron pairs in low-bandgap polymers for photovoltaics. *Nat Commun* **2012**, *3*, 970.
- 51. Aryanpour, K.; Sheng, C. X.; Olejnik, E.; Pandit, B.; Psiachos, D.; Mazumdar, S.; Vardeny, Z. V., Evidence for excimer photoexcitations in an ordered pi-conjugated polymer film. *Physical Review B* **2011**, *83* (15).
- 52. Song, Y.; Schubert, A.; Liu, X.; Bhandari, S.; Forrest, S. R.; Dunietz, B. D.; Geva, E.; Ogilvie, J. P., Efficient Charge Generation via Hole Transfer in Dilute Organic Donor-Fullerene Blends. *J Phys Chem Lett* **2020**, *11* (6), 2203-2210.
- 53. Mani, T.; Grills, D. C.; Newton, M. D.; Miller, J. R., Electron Localization of Anions Probed by Nitrile Vibrations. *J Am Chem Soc* **2015**, *137* (34), 10979-91.
- 54. Mani, T.; Grills, D. C., Probing Intermolecular Electron Delocalization in Dimer Radical Anions by Vibrational Spectroscopy. *J Phys Chem B* **2017**, *121* (30), 7327-7335.
- 55. Ferguson, A. J.; Kopidakis, N.; Shaheen, S. E.; Rumbles, G., Quenching of excitons by holes in poly(3-hexylthiophene) films. *J Phys Chem C* **2008**, *112* (26), 9865-9871.
- 56. Hodgkiss, J. M.; Albert-Seifried, S.; Rao, A.; Barker, A. J.; Campbell, A. R.; Marsh, R. A.; Friend, R. H., Exciton-Charge Annihilation in Organic Semiconductor Films. *Adv Funct Mater* **2012**, *22* (8), 1567-1577.
- 57. Stallhofer, K.; Nuber, M.; Kienberger, R.; Körstgens, V.; Müller-Buschbaum, P.; Iglev, H., Dynamics of Short-Lived Polaron Pairs and Polarons in Polythiophene Derivatives Observed via Infrared-Activated Vibrations. *The Journal of Physical Chemistry C* **2019**, *123* (46), 28100-28105.
- 58. Kovalenko, S. A.; Dobryakov, A. L.; Ruthmann, J.; Ernsting, N. P., Femtosecond spectroscopy of condensed phases with chirped supercontinuum probing. *Phys Rev A* **1999**, *59* (3), 2369-2384.
- 59. Song, Y.; Schubert, A.; Maret, E.; Burdick, R. K.; Dunietz, B.; Geva, E.; Ogilvie, J., Vibronic structure of photosynthetic pigments probed by polarized two-dimensional electronic spectroscopy and ab initio calculations. *Chemical Science* **2019**, (10), 8143-8153.
- 60. Di Nuzzo, D.; Viola, D.; Fischer, F. S.; Cerullo, G.; Ludwigs, S.; Da Como, E., Enhanced Photogeneration of Polaron Pairs in Neat Semicrystalline Donor-Acceptor Copolymer Films via Direct Excitation of Interchain Aggregates. *J Phys Chem Lett* **2015**, *6* (7), 1196-203.
- 61. Zaikowski, L.; Kaur, P.; Gelfond, C.; Selvaggio, E.; Asaoka, S.; Wu, Q.; Chen, H. C.; Takeda, N.; Cook, A. R.; Yang, A.; Rosanelli, J.; Miller, J. R., Polarons, bipolarons, and side-by-side polarons in reduction of oligofluorenes. *J Am Chem Soc* **2012**, *134* (26), 10852-63.
- 62. Zamadar, M.; Asaoka, S.; Grills, D. C.; Miller, J. R., Giant infrared absorption bands of electrons and holes in conjugated molecules. *Nat Commun* **2013**, *4* (2818), 1-7.
- 63. Chekalin, S. V.; Yartsev, A. P.; Sundstrom, V., Generation of charge carriers in C60 films by 100-fs laser pulses with photon energies above and below the mobility edge. *Quantum Electron+* **2001**, *31* (5), 395-397.
- 64. Kazaoui, S.; Minami, N.; Tanabe, Y.; Byrne, H. J.; Eilmes, A.; Petelenz, P., Comprehensive analysis of intermolecular charge-transfer excited states in C₆₀ and C₇₀ films. *Physical Review B* **1998**, *58* (12), 7689-7700.